ACS Photonics

Article

pubs.acs.org/journal/apchd5

Tunable Out-of-Plane Excitons in 2D Single-Crystal Perovskites

Antonio Fieramosca,[†,‡] Luisa De Marco,[*,†] Marco Passoni,[¶] Laura Polimeno,[†,‡] Aurora Rizzo,[†] Barbara L. T. Rosa,[§] Giuseppe Cruciani,[∥] Lorenzo Dominici,[†] Milena De Giorgi,[†] Giuseppe Gigli,[†] Lucio C. Andreani,[¶] Dario Gerace,[*,¶] Dario Ballarini,[*,†] and Daniele Sanvitto[†,⊥]

[†]CNR NANOTEC Institute of Nanotechnology, Via Monteroni, 73100 Lecce, Italy

[‡]Dipartimento di Matematica e Fisica, Universitá del Salento, Via Arnesano, 73100 Lecce, Italy

[¶]Dipartimento di Fisica, Universitá degli Studi di Pavia, Via Bassi 6, 27100 Pavia, Italy

[§]Universidade Federal de Minas Gerais, Avenida Presidente Antonio Carlos 6627, 31270901, Belo Horizonte, Brazil

[∥]Department of Physics and Earth Sciences, University of Ferrara, Via G. Saragat 1, I-44122 Ferrara, Italy

[⊥]INFN Istituto Nazionale di Fisica Nucleare, Sezione di Lecce, 73100 Lecce, Italy

S *Supporting Information*

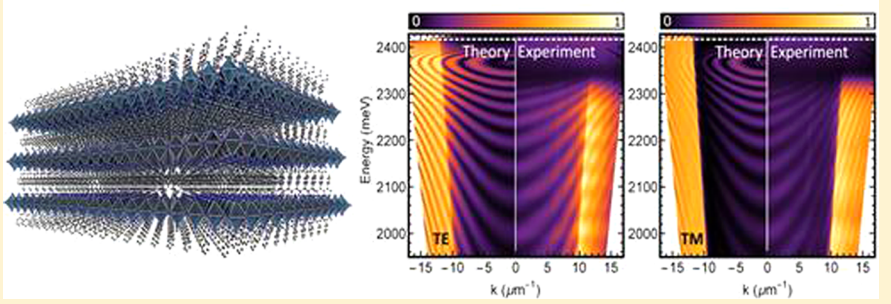

ABSTRACT: Hybrid organic−inorganic perovskites have emerged as very promising materials for photonic applications, thanks to the great synthetic versatility that allows tuning their optical properties. In the two-dimensional (2D) crystalline form, these materials behave as multiple-quantum-well heterostructures with stable excitonic resonances up to room temperature. In this work strong light−matter coupling in 2D perovskite single-crystal flakes is observed, and the polarization-dependent exciton−polariton response is used to disclose new excitonic features. For the first time, an out-of-plane component of the excitons is observed, unexpected for such 2D systems and completely absent in other layered materials such as transition-metal dichalcogenides. By comparing different hybrid perovskites with the same inorganic layer but different organic interlayers, it is shown how the nature of the organic ligands controllably affects the out-of-plane exciton−photon coupling. Such vertical dipole coupling is particularly sought in those systems such as plasmonic nanocavities in which the direction of the field is usually orthogonal to the material sheet. Organic interlayers are shown to affect also the strong birefringence associated with the layered structure, which is exploited in this work to completely rotate the linear polarization degree in only a few micrometers of propagation: akin to what happens in metamaterials.

KEYWORDS: *layered perovskites, light−matter coupling, exciton−polaritons, anisotropy, birefringence, hybrid semiconductors*

Two-dimensional (2D) semiconductors are attracting increasing attention, due to both their relevance in quantum optoelectronics and their complex physical properties, still not fully unraveled. In addition to many single-layer systems, such as transition-metal dichalcogenides (TMD), graphene, and its inorganic analogues, hybrid 2D organic−inorganic perovskites offer a valuable alternative because they may be represented as natural realizations of multiple-quantum-well (QW) heterostructures, with outstanding optical properties at room temperature.[1−5] Layered 2D perovskites generally consist of an inorganic layer of $[PbX_6]^{2-}$ octahedra (with the halogen X = Cl, Br, or I) sandwiched between bilayers of intercalated alkylammonium cations (see, for example, Figure 1a). The lowest-energy electronic excitations are associated with the inorganic sheet, while the organic part is believed to behave as a potential barrier.[2] Therefore, these crystalline materials combine the advantages of organics, such as the easy and cheap manufacturing, and those possessed by inorganic compounds, i.e., robustness and excellent optical properties.[6] Moreover, by changing the inorganic precursors it is possible to tune the band gap in a wide energy range, while the choice of the organic component can tailor the QW-type structure to a large extent. As compared to epitaxially grown GaAs-based QW heterostructures, for instance, these materials allow for higher dielectric confinement and larger binding

Received: July 18, 2018
Published: September 11, 2018

DOI: 10.1021/acsphotonics.8b00984
ACS Photonics XXXX, XXX, XXX−XXX

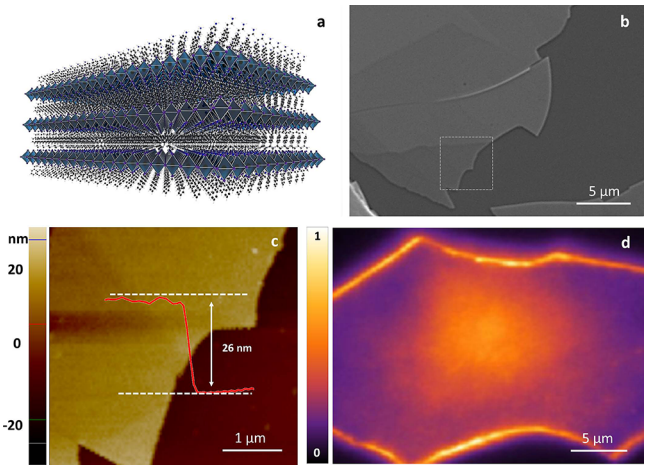

Figure 1. (a) Schematic illustration of the layered perovskite crystal structures; (b) SEM image of a $(PEAI)_2PbI_4$ exfoliated crystal; (c) AFM topography image of the white dashed square indicated in (b) with the corresponding height profile; (d) Real-space photoluminescence of a $(PEAI)_2PbI_4$ perovskite crystal.

energies. As a further advantage over TMD monolayers, 2D hybrid perovskites display enhanced collective effects due to the large number of layers stacked in a single crystal without the problem of moving toward an indirect band gap typical of bulk TMDs.

These peculiar properties make layered 2D perovskites not only an interesting system to be investigated per se but also ideal candidates for the development of novel optoelectronic devices to efficiently control photonic signals.[7−9] Particularly interesting is the use of 2D perovskites as active layers for strong light−matter coupling with the consequent generation of exciton−polariton quasiparticle.[10,11]

Indeed, evidence for exciton−polariton effects has been reported, although only in polycrystalline 2D hybrid perovskite thin films embedded in mirror microcavities[12−17] and recently in all-inorganic perovskite $CsPbCl_3$ nanoplatelets optically confined between two distributed Bragg reflectors.[18]

Here, we observe strong exciton−photon coupling in 2D hybrid perovskite single-crystal waveguides, avoiding the need to embed them within mirror microcavities, and we use polarization-dependent exciton−polariton response to investigate their excitonic properties. Taking advantage of their strong light−matter coupling, we assess the nature of the elementary excitations of these systems, and varying the polarization of the incident electromagnetic radiation, we probe the in-plane and out-of-plane excitonic response. Surprisingly, for the first time we disclose a polariton response associated with an out-of-plane excitonic component, which was somehow unexpected in such 2D structures.

This observation was possible thanks to the use of large single crystal flakes of 2D perovskite that are employed to directly measure the excitonic response without being limited by nonradiative losses and grain-to-grain heterogeneity or tilt boundaries, usually present in polycrystalline films.

The dual nature of 2D perovskite excitons is also independently confirmed by far-field polarized photoluminescence measurements, which allow us to assess the in-plane and out-of-plane components of the exciton transition momentum dipole.

Moreover, to investigate the origin of this behavior, we produce 2D layered crystalline perovskites with the same inorganic part but different organic ligands, and we observe that the dual-exciton features are related to the inter-QW distance and layer structure showing that the choice of the organic component provides a new route to control not only the energy but also the orientation and polarization of the transition dipole in these hybrid perovskites.

Finally, we measure the optical anisotropy due to the layered electronic structure akin to a metamaterial, finding that the choice of organic interlayer sensitively alters the polarized optical response. We observe large intrinsic birefringence in our monocrystalline flakes, and we demonstrate the use of them as half-waveplates with thicknesses of a few optical periods.

RESULTS

We produce large thin crystals of 2D hybrid perovskite by an antisolvent vapor-assisted crystallization method recently reported[19] and subsequent mechanical exfoliation. We synthesize three different layered perovskites changing the organic precursors: we select two alkyl cations, butylammonium $(C_4H_9NH_3)_2PbI_4$ (BAI) and octylammonium $(C_8H_{17}NH_3)_2PbI_4$ (OCT), having different chain lengths in order to tune the distance between the inorganic layers; in addition we introduce an aromatic moiety, phenethylammonium $(C_6H_5(CH_2)_2NH_3)_2PbI_4$ (PEAI), to investigate its effect on the exciton−photon coupling. Further details about their synthesis and their structures are provided in the Supporting Information.

The unit cell parameters verified by X-ray diffraction measurements (see Figure S1 and Table S1 in the Supporting Information) allow the determination of the thicknesses of barrier and well in the multi-QW structure: the inorganic semiconductor layer is 0.64 nm thick, while the organic interlayer is 0.75, 1.02, and 1.24 nm thick for BAI, PEAI, and OCT, respectively (see Table 1 and Table S1). The exfoliated flakes observed by scanning electron microscopy (SEM) and atomic force microscopy (AFM), shown in Figure 1b,c (see also Figures S2 and S3 in the Supporting Information), reveal terrace structures with the planes oriented parallel to the

Table 1. Parameters Obtained from the Comparison between Numerical Simulations and Experimental Data for the Three Different Types of Layered 2D Perovskite Films Considered

	BAI	PEAI	OCT
Organic ligand	Aliphatic 	Aromatic 	Aliphatic 
Organic layer thickness	0.75nm	1.02nm	1.24nm
Δn	0.15	0.1	0.2
% OP	18 %	16 %	10 %
f_{osc} IP	$6.1{\cdot}10^{13}$ cm^{-2}	$4.4{\cdot}10^{13}$ cm^{-2}	$5.3{\cdot}10^{13}$ cm^{-2}
Coupling strength	240 meV	170 meV	250 meV
Exciton FWHM	52 meV	33 meV	44 meV

DOI: 10.1021/acsphotonics.8b00984
ACS Photonics XXXX, XXX, XXX−XXX

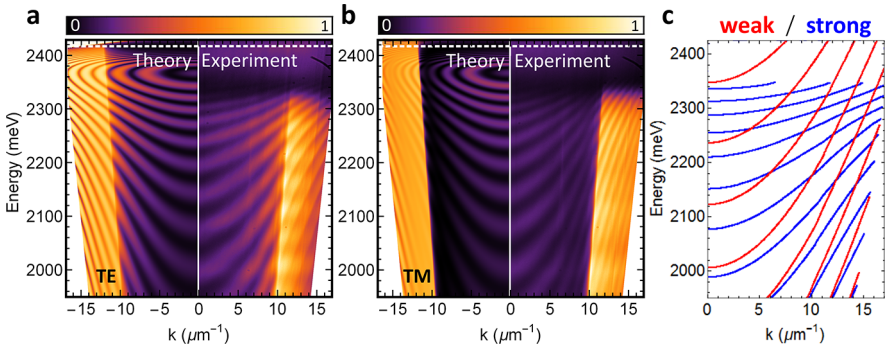

Figure 2. Reflection spectra are plotted as energy versus in-plane momentum, k, with $k = \frac{2\pi}{\lambda}\sin\theta$, where λ is the wavelength and θ the incidence angle. Multiple resonances are due to the Fabry−Perot configuration, with the enhanced intensity corresponding to angles of incidence beyond the air−light line. Reflectivity maps measured (right half-panel) and calculated by scattering matrix (left half-panel) for an OCT single crystal under white light illumination for (a) TE and (b) TM polarizations are shown in the left and right column, respectively. (c) Reflection minima calculated with (blue lines) and without (red lines) the excitonic resonance, showing the crucial modification of the reflection spectrum induced by strong light−matter interaction as compared to a bare film response. The white dashed lines indicate the exciton energy position. The black band close to the exciton resonance is due to the presence of multiple polariton modes that red-shift the absorption peak energy below the excitonic resonance due to the significant Rabi splitting in the strong coupling regime.

substrate. All samples show an extremely uniform photoluminescence (see Figure 1d) that, differently from the majority of the reported studies carried out on polycrystalline films, is not affected by the presence of intergrain voids or grain boundaries (see also Figure S4 in the Supporting Information). In a single crystal we can notice that the bright regions in the PL emission observed along the boundaries of the flake are due to scattering of the guided radiation with defects at the edges of the film, while the rest of the crystal is very uniform and defect-free including the excitation spot which is rather brighter in the central part of the flake. Absorption and photoluminescence (PL) spectra taken on thin single-crystal flakes are shown in the Supporting Information (Figure S5).

The optical response of single crystals of BAI, PEAI, and OCT with thicknesses of a few micrometers is investigated with an oil-immersion objective (details are reported in the Supporting Information) that allows the capture, from the glass substrate side, of also the signal beyond the air−light line, i.e., the signal coming from total internal reflection (TIR) at the crystal−air interface. Both PL and reflection spectra (see Figure 2a,b and also Figure S6 and Figure S7 in the Supporting Information) show the frequency modulation due to partial reflection on the crystal−substrate (glass) interface and to TIR at the crystal−air interface for angles larger than $\theta = \arcsin\frac{n_{air}}{n_{glass}} \approx 40°$, where $n_{air/glass}$ is the refractive index of air (or substrate, respectively). The figure shows the typical dispersion of strong light−matter coupling, with the optical resonances bending close to the excitonic resonance at large angles. A considerable amount of information about the nature of the elementary excitations in these compounds can be inferred by analyzing the material response to optically exciting polarizations with either the electric field (TE, Figure 2a) or the magnetic field (TM, Figure 2b) transversely oriented with respect to the incidence plane. Indeed, for TE-polarized light, only the dipoles oriented in the plane of the QW (associated with the $[PbX_6]^{2-}$ inorganic sheets) contribute to the material polarizability, while both in-plane (IP) and out-of-plane (OP) dipole strengths have to be considered when looking at the response in TM polarization. By comparing the experimental data (right side of each panel in Figure 2) with numerical simulations (left side of each panel in Figure 2), we are able to obtain a quantitative estimation on the exciton dipole orientation in these materials. Figure 2c shows the mode dispersions in the strong- and weak-coupling regime. In the weak-coupling regime, the medium has been simulated without Lorentzian response by using the background index as indicated in Figure S10 in the Supporting Information. The striking difference of the mode dispersion when including the effect of strong light−matter interaction is clearly evident close to the excitonic resonance.

The optical response of the 2D perovskite films is modeled with a generalized scattering matrix algorithm,[20−22] which allows simultaneously including both the natural birefringence of the stacked organic−inorganic layers and the polarization-dependent exciton response. Details about the theoretical method and the implementation used in this work are reported in the Supporting Information. In principle, this system would be amenable to simulation with transfer matrix approaches properly extended to include the anisotropic dielectric response of the material,[23−25] although our modeling proved essential to capture the key ingredients of such peculiar systems, especially in terms of numerical stability toward the inclusion of absorption losses. Thanks to this analysis, we have selected the values that allow us to best describe the qualitative and quantitative behavior of the different layered materials, as summarized in Table 1. Doing so, we can demonstrate that the optical response of these materials is determined from doubly polarized excitonic contributions, corresponding to optically active dipoles oscillating both in and out of the inorganic layers plane. This is surprising, since these materials are considered 2D semiconductors with excitons strongly confined between insulating barriers. Nevertheless, the vertical contribution is crucial to correctly capture the reflectivity spectra detected in TM polarization with out-of-plane oscillating dipoles, contributing significantly to the oscillator strength of the radiation−matter coupling, although by a generally smaller amount as compared to the in-plane oscillating dipoles (see quantitative estimate in Table 1). In addition, we observe that the out-of-plane oscillator strength decreases on increasing the organic barrier thickness between the inorganic perovskite layers (see the values obtained for BAI, PEAI, and OCT in Table 1): longer organic chains seem to lead to a stronger

DOI: 10.1021/acsphotonics.8b00984
ACS Photonics XXXX, XXX, XXX−XXX

confinement in the QW plane, with the exception of benzene rings, which slightly enhance the out-of-plane polarizability and strongly reduce the optical birefringence with respect to aliphatic chains of similar length.

To further corroborate the quantitative estimate of an out-of-plane component to the exciton−polariton response, we use Fourier-resolved, polarized photoluminescence measurements on a thin PEAI single crystal of 20 nm.

This is an effective technique to obtain the IP and OP contributions for thin films.[26,27] The Fourier plane of the vertical polarization is imaged in Figure 3a. For the emission

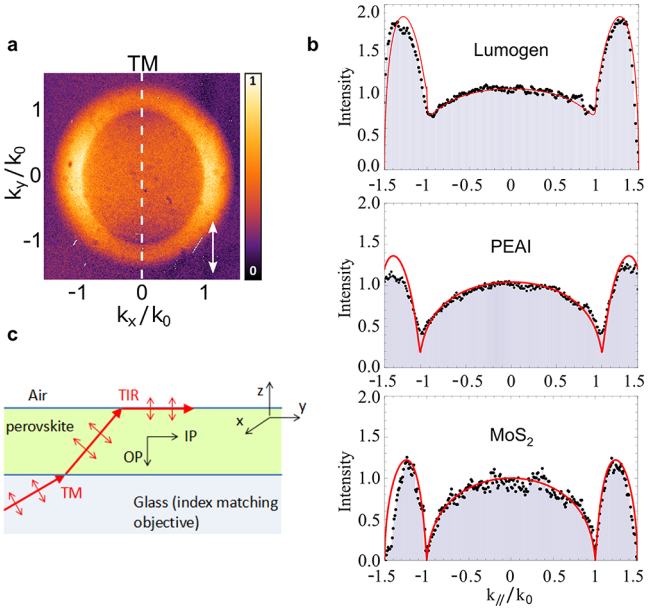

Figure 3. (a) 2D Fourier space emission (PL) in the linear vertical polarization (white arrow). The white dashed line represents the TM section, in which the OP contribution is distinguished at the TIR angle (corresponding to k_0 for each material). (b) PL signal along the white dashed line in (a) for isotropic material (Lumogen), thin crystal 2D perovskite (PEAI), and MoS_2 monolayer. (c) Scheme representing the vanishing local optical density of states at $k_{||}/k_0 = 1$ for out-of-plane dipoles in vertical polarization. In the TM plane, the OP fraction is 50%, 30%, and 0% for Lumogen, PEAI, and b_2, respectively. These values correspond, in the 3D volume, to an OP contribution of 33% for the isotropic case and 18% for the PEAI.

direction along k_y, the local density of optical states is completely suppressed close to the TIR direction for IP polarization, and the OP contribution can be isolated. In Figure 3b, the results for the PEAI crystal are compared with a MoS_2 monolayer (fully in-plane excitons) and with an isotropic molecular thin film (Lumogen Orange, 35 nm). The fitting functions are obtained by following the analytic model in refs 26 and 27 and using an OP fraction of (33 ± 5)% for the isotropic case and <5% for MoS_2 monolayer. According to the results of simulations in Figure 2, we consider an OP fraction of (18 ± 5)% for the PEAI thin film, obtaining an overall good agreement with both the experimental results and the scattering matrix analysis. This measurement independently confirms the presence of out-of-plane oscillating dipoles and thus the double nature of 2D perovskite excitons.

These results show two particularly relevant aspects: on one hand, we clearly evidence a polarization-dependent and anisotropic (i.e., possessing an OP dipolar component) exciton response; on the other hand we see a barrier-dependent oscillator strength. Both these effects are unexpected at first sight, since up to now electronic band structure calculations have predicted an ideally perfect in-plane orientation of the exciton momentum dipole due to the high energy barrier (∼1 eV) of the organic layer. This is evidence that the role of the organic ligands had been downplayed in these compounds.[28]

As a matter of fact, it is well established that the elementary excitations in these layered materials should arise from optical transitions coming from half-integer total angular momentum valence band states ($j = 1/2$, $m_j = \pm 1/2$, of Pb-6s orbitals) into conduction band states with the same j,m_j symmetry (mainly arising from Pb-6p orbitals; see, for example, refs 29−31). This is quite different from what happens in inorganic QWs, i.e., III−V semiconductors, in which heavy-hole excitons represent the lowest energy transitions from $j = 3/2$ (p-type) valence band to $j = 1/2$ (s-type) conduction band states. While these latter transitions lead to strictly in-plane polarized states (see, for example, ref 32), in the case of 2D perovskites—due to polarization selection rules derived from dipole matrix elements—vertically polarized transitions are permitted.

Our observations suggest that the organic interlayer could actually play a non-negligible role beyond that of a passive insulating barrier. Moreover, the dielectric constant of the organic part, its thickness, and its energy levels could affect the interactions between the excitons of the semiconducting inorganic layers and thus their response to a given polarization of the incident radiation.[1] These hypotheses are only speculative and worth being investigated in detail, e.g., through microscopic theories of the optical response that the present work will hopefully stimulate.

Regarding the interest in these results for polaritonic applications, we observe that the values of the exciton oscillator strength per unit surface (reported in Table 1) are fully consistent with the strong coupling regime in all of the perovskite samples considered so far. In particular, the radiation−matter coupling energy can be obtained by the usual expression employed for bulk exciton−polaritons, which is expressed as[33]

$$E_c = \hbar\Omega_c = \hbar\sqrt{\frac{e^2}{4\varepsilon_0\varepsilon_r m_0}\frac{f}{V}} \quad (1)$$

where e is the elementary electric charge, m_0 is the free electron mass, and ε_r is the background dielectric permittivity relative to the vacuum, ε_0. Here, the 2D nature of the elementary excitations in each perovskite layer is combined with the multi-QW-type structure, which is interpreted as an effective medium with oscillator strength per unit volume $f/V = (f/S)/d$, where d is the thickness of the active organic plus the inorganic barrier layers in each of the perovskite compounds considered. The estimated coupling strengths for the BAI, PEAI, and OCT materials (see Table 1) show values that are compatible with very large light−matter coupling regimes; in particular the condition $\hbar\Omega_c >$ fwhm is fully satisfied in all three cases. We also notice that these values are especially remarkable when compared to standard III−V semiconductor heterostructures, in which radiation−matter coupling energy is typically measured on the order of a few meV while the coupling strength is on the order of 200 meV in our case, although care should be taken when comparing these values of Rabi coupling since typical experiments in fully inorganic semiconductors are performed with single or few III−V

DOI: 10.1021/acsphotonics.8b00984
ACS Photonics XXXX, XXX, XXX−XXX

quantum wells. In particular, the present experiments correspond in spirit to early investigations on the optical response of thin films in III−V semiconductors with strong excitonic absorption,[34−36] where exciton−polariton effects were first evidenced even in the absence of bottom and top mirrors.

Finally, we take advantage of the surface homogeneity of these monocrystalline slabs to illustrate optical propagation for distances of tens of micrometers without being scattered by defects (see Figure 4a and Figure S9 in the Supporting Information). An additional advantage of the large extension of the single crystals is the possibility to exploit the large optical birefringence induced by the layered material structure, akin to that of metamaterials. Interestingly, black phosphorus has been recently proposed for fabrication of atomically thin optical waveplates thanks to its in-plane birefringence as high as $\Delta n \approx 0.245$.[37] Here we measure the dispersion of the refractive index along and perpendicular to the layer structure in the transparent region of the spectrum for PEAI, BAI, and OCT (see Figure S11 in the Supporting Information), finding comparable values ($\Delta n \approx 0.2$ for OCT, see Table 1). However, compared to the black phosphorus, the 2D perovskites show an out-of-plane birefringence that can be tuned by the choice of the organic ligand either by changing the interlayer separation or by exploiting the organic−inorganic nature of higher electronic levels in the presence of short interlayer distances or π-conjugated organic systems (see the effect of benzene rings on optical anisotropy in Table 1). Here, as a demonstration, we show that such a huge optical anisotropy can be effectively used as an ultrathin waveplate. For light traveling with a finite angle, with respect to the direction normal to the structure, the retardation between the components of the electromagnetic field oscillating in- and out-of-plane is large enough to result in a complete rotation of the linear polarization degree in few optical periods. In Figure 4b, the angle of incidence is chosen beyond the light-line in air to detect the totally reflected signal at the TIR interface, allowing the measurement of a complete rotation of the linear polarization degree for a crystal thickness of just 1 μm. In inorganic microcavities, the optical and excitonic anisotropies are enhanced under a strong coupling regime, giving rise to strong spin−orbit effective interactions for polaritons propagating in the plane of the structure. These results indicate that self-assembled waveguides of 2D layered perovskites can be a promising system to study the effects of the strong optical anisotropy on the spin dynamics of exciton−polaritons and can be used as integrated waveplates in optical circuits, as well as in polariton-based devices.

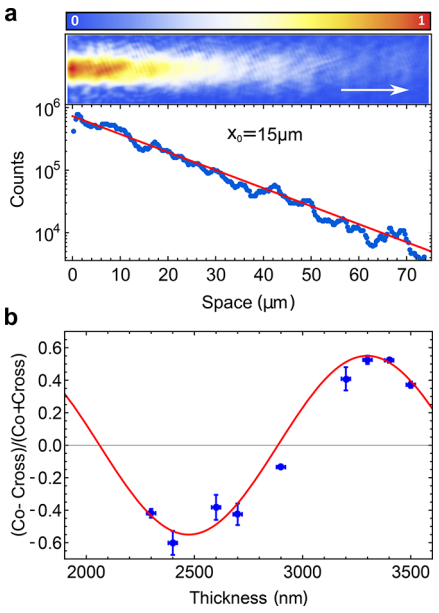

Figure 4. (a) Real space intensity image of a resonant injected beam in a PEAI crystal. (b) Rotation of the linear polarization degree in a set of PEAI crystals with a birefringence of $\Delta n = 0.1$. A continuous wave laser at 640 nm with diagonal polarization (mixed TE and TM) is focused by the oil-immersion objective beyond the angle of TIR at the air interface. The co- and cross-polarized reflected beam is measured for different slab thicknesses, and the linear polarization degree is fitted with a sinusoidal function.

In summary, we have shown that 2D perovskites possess dual excitonic properties that can be tuned by the choice of the organic cations, which in turn affect the exciton confinement and its optical response, in terms of both the out-of-plane component of the transition dipole moment and the intrinsic birefringence of the structure. The presence of a hybrid organic and inorganic structure in 2D perovskites provides an ideal platform for developing novel multifunctional materials in which the crystalline architectures can be synthetically fine-tuned in order to provide a huge range of semiconductors with different properties. These observations pave the way for the design and fabrication of all-optical devices based on 2D perovskites.

■ ASSOCIATED CONTENT

Supporting Information

The Supporting Information is available free of charge on the ACS Publications website at DOI: 10.1021/acsphotonics.8b00984.

Experimental details; XRD characterizations; supplementary SEM and AFM images for exfoliated crystals; PL images of PEAI polycrystalline film and single-crystal flake; absorption and emission spectra for BAI, PEAI, and OCT; supplementaty reflection spectra; simulation details; ellispometric measurements (PDF)

■ AUTHOR INFORMATION

Corresponding Authors

*E-mail: luisa.demarco@nanotec.cnr.it.
*E-mail: dario.gerace@unipv.it.
*E-mail: dario.ballarini@nanotec.cnr.it.

ORCID

Luisa De Marco: 0000-0002-6855-5438
Aurora Rizzo: 0000-0002-4570-7777
Milena De Giorgi: 0000-0002-4522-7933

Author Contributions

A.F. and L.P. performed the optical measurements, and A.F., L.P., L.D.M., and B.L.T.R. prepared the material and the samples. M.P., L.C.A., and D.G. performed the numerical simulations, the theoretical modeling, and interpretation of data. G.C. performed X-ray measurements. L.D., M.D.G., A.R., and G.G. contributed to the experimental realization and interpretation of the results. L.D.M., D.G., D.B., and D.S. supervised the work.

DOI: 10.1021/acsphotonics.8b00984
ACS Photonics XXXX, XXX, XXX−XXX

Notes

The authors declare no competing financial interest.

■ ACKNOWLEDGMENTS

The authors acknowledge the ERC project ElecOpteR grant number 780757. G.G. gratefully acknowledges the project PERSEO-PERrovskite-based Solar cells: towards high Efficiency and lOng-term stability (Bando PRIN 2015-Italian Ministry of University and Scientific Research (MIUR) Decreto Direttoriale 4 novembre 2015 n. 2488, project number 20155LECAJ). A.R. gratefully acknowledges SIR "Two-Dimensional Colloidal Metal Dichalcogenides based Energy-Conversion Photovoltaics" (2D ECO), project number RBSI14-FYVD. The authors acknowledge Sonia Carallo for technical support and AFM measurements. The authors acknowledge Nitto Italia s.r.l. for providing the tape for mechanical exfoliation. D.S., D.B., A.F., and L.D.M. are grateful to Stéphane Kéna-Cohen and Fábio Barachati for fruitful discussions.

■ REFERENCES

(1) Pedesseau, L.; Sapori, D.; Traore, B.; Robles, R.; Fang, H.-H.; Loi, M. A.; Tsai, H.; Nie, W.; Blancon, J.-C.; Neukirch, A.; Tretiak, S.; Mohite, A. D.; Katan, C.; Even, J.; Kepenekian, M. Advances and Promises of Layered Halide Hybrid Perovskite Semiconductors. *ACS Nano* **2016**, *10*, 1936−0851.

(2) Saparov, B.; Mitzi, D. B. OrganicInorganic Perovskites: Structural Versatility for Functional Materials Design. *Chem. Rev.* **2016**, *116*, 4558−4596.

(3) Ha, S.-T.; Shen, C.; Zhang, J.; Xiong, Q. Laser cooling of organicinorganic lead halide perovskites. *Nat. Photonics* **2017**, *10*, 2598−2602.

(4) Sutherland, B. R.; Sargent, E. H. Perovskite photonic sources. *Nat. Photonics* **2016**, *10*, 295.

(5) Cortecchia, D.; Lew, K. C.; So, J.-K.; Bruno, A.; Soci, C. Cathodoluminescence of Self-Organized Heterogeneous Phases in Multidimensional Perovskite Thin Films. *Chem. Mater.* **2017**, *29*, 10088−10094.

(6) Gholipour, B.; Adamo, G.; Cortecchia, D.; Krishnamoorthy, H. N. S.; Birowosuto, M. D.; Zheludev, N. I.; Soci, C. Organometallic Perovskite Metasurfaces. *Adv. Mater.* **2017**, *29*, 1604268.

(7) Carusotto, I.; Ciuti, C. Quantum fluids of light. *Rev. Mod. Phys.* **2013**, *85*, 299−366.

(8) Byrnes, T.; Kim, N. Y.; Yamamoto, Y. Excitonpolariton condensates. *Nat. Phys.* **2014**, *10*, 803−813.

(9) Sanvitto, D.; Kéna-Cohen, S. The road towards polaritonic devices. *Nat. Mater.* **2016**, *15*, 1061−1073.

(10) Weisbuch, C.; Nishioka, M.; Ishikawa, A.; Arakawa, Y. Observation of the coupled exciton-photon mode splitting in a semiconductor quantum microcavity. *Phys. Rev. Lett.* **1992**, *69*, 3314−3317.

(11) Sun, Y.; Wen, P.; Yoon, Y.; Liu, G.; Steger, M.; Pfeiffer, L. N.; West, K.; Snoke, D. W.; Nelson, K. A. Bose−Einstein Condensation of Long-Lifetime Polaritons in Thermal Equilibrium. *Phys. Rev. Lett.* **2017**, *118*, 016602.

(12) Fujita, T.; Sato, Y.; Kuitani, T.; Ishihara, T. Tunable polariton absorption of distributed feedback microcavities at room temperature. *Phys. Rev. B: Condens. Matter Mater. Phys.* **1998**, *57*, 12428−12434.

(13) Brehier, A.; Parashkov, R.; Lauret, J. S.; Deleporte, E. Strong exciton-photon coupling in a microcavity containing layered perovskite semiconductors. *Appl. Phys. Lett.* **2006**, *89*, 171110.

(14) Wenus, J.; Parashkov, R.; Ceccarelli, S.; Brehier, A.; Lauret, J.-S.; Skolnick, M. S.; Deleporte, E.; Lidzey, D. G. Hybrid organic-inorganic exciton-polaritons in a strongly coupled microcavity. *Phys. Rev. B: Condens. Matter Mater. Phys.* **2006**, *74*, 235212.

(15) Lanty, G.; Bréhier, A.; Parashkov, R.; Lauret, J. S.; Deleporte, E. Strong excitonphoton coupling at room temperature in microcavities containing two-dimensional layered perovskite compounds. *New J. Phys.* **2008**, *10*, 065007.

(16) Lanty, G.; Lauret, J. S.; Deleporte, E.; Bouchoule, S.; Lafosse, X. UV polaritonic emission from a perovskite-based microcavity. *Appl. Phys. Lett.* **2008**, *93*, 081101.

(17) Niu, W.; Ibbotson, L. A.; Leipold, D.; Runge, E.; Prakash, G. V.; Baumberg, J. J. Image excitons and plasmon-exciton strong coupling in two-dimensional perovskite semiconductors. *Phys. Rev. B: Condens. Matter Mater. Phys.* **2015**, *91*, 91.

(18) Su, R.; Diederichs, C.; Wang, J.; Liew, T. C. H.; Zhao, J.; Liu, S.; Xu, W.; Chen, Z.; Xiong, Q. Room-Temperature Polariton Lasing in All-Inorganic Perovskite Nanoplatelets. *Nano Lett.* **2017**, *17*, 3982−3988.

(19) Ledee, F.; Trippe-Allard, G.; Diab, H.; Audebert, P.; Garrot, D.; Lauret, J.-S.; Deleporte, E. Fast growth of monocrystalline thin films of 2D layered hybrid perovskite. *CrystEngComm* **2017**, *19*, 2598−2602.

(20) Li, L. Formulation and comparison of two recursive matrix algorithms for modeling layered diffraction gratings. *J. Opt. Soc. Am. A* **1996**, *13*, 1024−1035.

(21) Whittaker, D. M.; Culshaw, I. S. Scattering-matrix treatment of patterned multilayer photonic structures. *Phys. Rev. B: Condens. Matter Mater. Phys.* **1999**, *60*, 2610−2618.

(22) Liscidini, M.; Gerace, D.; Andreani, L. C.; Sipe, J. E. Scattering-matrix analysis of periodically patterned multilayers with asymmetric unit cells and birefringent media. *Phys. Rev. B: Condens. Matter Mater. Phys.* **2008**, *77*, 035324.

(23) Andreani, L. C. Exciton-polaritons in superlattices. *Phys. Lett. A* **1994**, *192*, 99−109.

(24) Vladimirova, M. R.; Kavokin, A. V.; Kaliteevski, M. A. Dispersion of bulk exciton polaritons in a semiconductor microcavity. *Phys. Rev. B: Condens. Matter Mater. Phys.* **1996**, *54*, 14566−14571.

(25) Lerario, G.; Cannavale, A.; Ballarini, D.; Dominici, L.; Giorgi, M. D.; Liscidini, M.; Gerace, D.; Sanvitto, D.; Gigli, G. Room temperature Bloch surface wave polaritons. *Opt. Lett.* **2014**, *39*, 2068−2071.

(26) Schuller, J. A.; Karaveli, S.; Schiros, T.; He, K.; Yang, S.; Kymissis, I.; Shan, J.; Zia, R. Orientation of luminescent excitons in layered nanomaterials. *Nat. Nanotechnol.* **2013**, *8*, 271−276.

(27) Scott, R.; Heckmann, J.; Prudnikau, A. V.; Antanovich, A.; Mikhailov, A.; Owschimikow, N.; Artemyev, M.; Climente, J. I.; Woggon, U.; Grosse, N. B.; Achtstein, A. W. Directed emission of CdSe nanoplatelets originating from strongly anisotropic 2D electronic structure. *Nat. Nanotechnol.* **2017**, *12*, 1155−1160.

(28) Even, J.; Pedesseau, L.; Dupertuis, M.-A.; Jancu, J.-M.; Katan, C. Electronic model for self-assembled hybrid organic/perovskite semiconductors: Reverse band edge electronic states ordering and spin-orbit coupling. *Phys. Rev. B: Condens. Matter Mater. Phys.* **2012**, *86*, 205301.

(29) Giovanni, D.; Chong, W. K.; Dewi, H. A.; Thirumal, K.; Neogi, I.; Ramesh, R.; Mhaisalkar, S.; Mathews, N.; Sum, T. C. Tunable room-temperature spin-selective optical Stark effect in solution-processed layered halide perovskites. *Sci. Adv.* **2016**, *2*, e1600477.

(30) Yu, Z. G. Effective-mass model and magneto-optical properties in hybrid perovskites. *Sci. Rep.* **2016**, *6*, 28576.

(31) Umebayashi, T.; Asai, K.; Kondo, T.; Nakao, A. Electronic structures of lead iodide based low-dimensional crystals. *Phys. Rev. B: Condens. Matter Mater. Phys.* **2003**, *67*, 155405.

(32) Yu, P. Y.; Cardona, M. *Fundamentals of Semiconductors*; Springer, 2010.

(33) Auffèves, A.; Gerace, D.; Richard, M.; Portolan, S.; Santos, M. F.; Kwek, L. C.; Miniatura, C. *Strong Light-Matter Coupling*; World Scientific Publishing Company, 2013.

(34) Chen, Y.; Bassani, F.; Massies, J.; Deparis, C.; Neu, G. Interference of the Exciton-Polariton Waves in GaAs Thin Layers. *EPL (Europhysics Letters)* **1991**, *14*, 483.

(35) Tredicucci, A.; Chen, Y.; Bassani, F.; Massies, J.; Deparis, C.; Neu, G. Center-of-mass quantization of excitons and polariton

DOI: 10.1021/acsphotonics.8b00984
ACS Photonics XXXX, XXX, XXX−XXX

interference in GaAs thin layers. *Phys. Rev. B: Condens. Matter Mater. Phys.* **1993**, *47*, 10348−10357.
(36) Boemare, C.; Gil, B.; Assunçao, M.; Sollner, J.; Taudt, W.; Heuken, M.; Nazare, M. H. Observation of Fabry-Pérot modes in the upper branch of the polariton in ZnSe-GaAs epilayers. *Phys. Rev. B: Condens. Matter Mater. Phys.* **1995**, *51*, 7954−7957.
(37) Yang, H.; Jussila, H.; Autere, A.; Komsa, H.-P.; Ye, G.; Chen, X.; Hasan, T.; Sun, Z. Optical Waveplates Based on Birefringence of Anisotropic Two-Dimensional Layered Materials. *ACS Photonics* **2017**, *4*, 3023−3030.

DOI: 10.1021/acsphotonics.8b00984
ACS Photonics XXXX, XXX, XXX−XXX